16th World Congress in Computational Mechanics (WCCM)
21-26 July 2024, Vancouver, Canada
A. Korobenko, M. Laforest, S. Prudhomme, R. Vaziri (Eds)

NON-DESTRUCTIVE STRESS WAVE AMPLITUDE TESTING FOR INTERFACE BONDING STRENGTH OF 3D PRINTABLE CONCRETE

CHENG QI*, YU-CHING WU AND PENG ZHI

College of Civil Engineering, Tongji University
1239 Siping Road, Shanghai 200092, China
qicheng@tongji.edu.cn

Key words: 3D printable concrete, Non-destructive testing, Interface properties, Stress wave.

Abstract. The aim of this study is to investigate the impact of interface bonding properties of 3D printable concrete (3DPC) on non-destructive testing. By fabricating concrete specimens with varying numbers of layers and employing ultrasonic devices for non-destructive testing, it was observed that the presence of interface layers results in 3DPC exhibiting smaller wave amplitudes compared to conventionally cast concrete. Moreover, with an increase in printing layers, there is a trend of initial growth followed by a decline in interface bonding strength, accompanied by changes in amplitude attenuation. Through the use of non-destructive testing methods and by observing the pattern of amplitude decay, the interface bonding properties of 3DPC were investigated. The results indicate that, compared to conventionally cast concrete, 3DPC prepared using additive manufacturing techniques significantly affects the propagation of stress waves due to interface layers, and there exists a linear relationship between interface bonding strength and wave amplitude loss. This may also be a fundamental factor contributing to differences in non-destructive testing outcomes.

1 INTRODUCTION

With the increasingly severe impact of the greenhouse effect on Earth, low-carbon environmental protection has become a major theme in the development of the times. 3D printable concrete (3DPC), as an emerging automated construction technology, has the ability to reduce the generation of construction waste. Therefore, it has sustainable development potential in the construction industry and is becoming a trend for the future.

However, compared to conventional cast concrete, due to the layered stacking construction method adopted by 3DPC, it will also exhibit mechanical anisotropy in the hardened state[1–8]. Currently, numerous studies have shown that interfacial bonding performance is the main factor affecting the anisotropy of 3DPC[9–15]. Research by Panda et al.[16,17] indicates that low strength is typically caused by weak bonds between printed filaments on the interface material, while studies by Roussel and Cussigh[18,19] suggest that during the layer-by-layer casting process of 3DPC, there is a short time for structure reconstruction in the first layer before the second layer of self-compacting concrete casting. If the reconstruction exceeds a critical yield stress value, the two layers cannot bond well together, resulting in weak interfaces between concrete layers.

In addition to printing time intervals, there are still many factors influencing the interfacial bonding performance of printed concrete. Keita et al.[20] demonstrated that a higher W/C ratio

is favorable for improving interfacial bond strength. Panda and Wolf[21], by controlling the distance between the extrusion layer and the nozzle, concluded that reducing the distance can significantly increase bond strength. Studies also indicate that different printing systems exhibit varying degrees of influence on pore characteristics (volume, shape, distribution, orientation). Kruger et al.[22] through experimentation observed that interface pores in printed concrete typically elongate and flatten along the printing direction, while in cast concrete, they are usually spherical, which is less conducive to stress concentration.

Ultrasonic technology is widely used in the non-destructive testing of concrete strength and defects. The propagation velocity of stress waves in concrete is a function of the solid Young's modulus, Poisson's ratio, density, and geometric shape. By understanding the relationship between the properties of concrete and the behavior of stress wave propagation, it is possible to infer relevant characteristics of the concrete by monitoring the propagation of stress waves. However, due to the presence of interface layers between the initial layers and subsequent layers in 3DPC, the propagation of stress waves differs from that in ordinary concrete.

Understanding the relationship between stress wave transmission and interfacial bonding properties in 3DPC is crucial for unifying non-destructive testing of 3DPC and conventional concrete. Therefore, this study printed concrete specimens with different numbers of layers and used an ultrasonic device to conduct inspections, comparing them with conventionally poured concrete. Experimental analysis was conducted to investigate the influence of the number of layers in 3DPC on interfacial bonding properties and stress wave transmission, and a theoretical model for stress wave propagation through printed concrete was established.

2 EXPERIMENTAL PROGRAMS

2.1 Materials and specimens

In this study, the base material used for 3D printing is fine aggregate concrete (FAC). The mix proportion of FAC is presented in Table 1, with natural sand serving as the fine aggregate, ordinary Portland cement (OPC) is used as the binder material, hydroxypropyl methylcellulose (HPMC) and nano clay (NC) are employed as rheological modifiers, sodium gluconate (SG) acts as a retarder, and polycarboxylate superplasticizer (SP) serves as a water reducer.

Table 1: Mix proportions of 3D-printed FAC (kg/m3)

OPC	NS	HPMC	NC	SP	SG	Water
1000	1000	1.28	5.63	0.7	0.7	350

Referring to previous studies, we define the printing direction as the *X*-axis, the direction perpendicular to the same horizontal plane as the *Y*-axis, and the deposition direction as the *Z*-axis. In this experiment, to simplify and control a single variable, concrete was printed in a single strip along the *Y*-axis. Therefore, the printed interface will only be in the middle layer. Two types of concrete specimens were cast: 100 mm cubic specimens and 100 × 100 × 300 mm prismatic specimens. Additionally, 6 types of 3DPC specimens were designed, with a printing strip width of 100 mm, a layer height of 10 mm, and a length of 400 mm. The variable was the number of layers in the 3DPC *n* (5, 6, 7, 8, 9, and 10 layers). Consequently, the dimensions of

the printed specimens were 400 × 100 × 10*n* mm. The specific experimental parameters are shown in Table ~~2~~2.

Table 2: Detailed characterizations of specimens

Specimen ID	Number of Print layers	Number of Interface Layers	Expected Height (mm)	Actual Height (mm)
C-100	-	-	100	100
C-300	-	-	300	300
3D-5	7	6	70	48
3D-6	4	3	40	57
3D-7	7	6	70	62
3D-8	8	7	80	76
3D-9	9	8	90	82
3D-10	10	9	100	95

In the specimen ID, "C" represents cast concrete, and the suffix indicates the concrete height in mm. "3D" represents 3DPC, and in "3D-*n*" the "*n*" denotes the number of printed layers. Due to the layer-by-layer deposition method used in 3DPC, the actual printed height is always lower than the expected height.

2.2 Test Setup

The ultrasonic tests were conducted after 28 days of curing. The schematic diagram of the non-destructive testing setup is shown in Figure 1. The 3DPC specimens had four measurement points, each spaced 100 mm apart. Non-metallic ultrasonic testing equipment was used to perform the tests at these points. The sampling interval was 0.4, the sampling length was 2048, and the emission voltage was 500V.

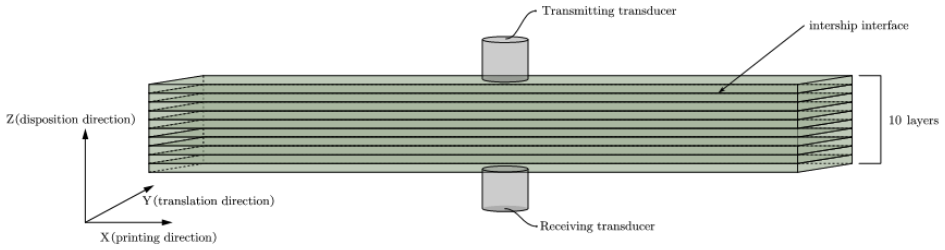

Figure 1: Schematic diagram of non-destructive testing

After completing the ultrasonic non-destructive testing, each 3D printed specimen was cut into blocks with interface dimensions of 10*n* × 100 mm. The bond strength of the interface was characterized using the split tensile strength test. The split tensile strength of the concrete was calculated according to the following equation:

$$f_{ts} = \frac{2F}{\pi A} = 0.637\frac{F}{A} \tag{1}$$

where F is the splitting load of the specimen, and A is the area of the splitting face of the specimen. For non-standard specimens, multiply by the corresponding size conversion factor.

3 THEORY AND RESULTS

3.1 Non-destructive testing of interface bond strength based on wave amplitude

Amplitude attenuation theory: When a stress wave propagates from material 1 to material 2, assuming the respective acoustic impedances are $\rho_1 c_1$ and $\rho_2 c_2$, due to the difference in their acoustic impedances, when the stress wave impinges on the interface, it will undergo transmission and reflection along the direction. The reflection coefficient R is given by the following equation:

$$R = \frac{\rho_2 c_2 - \rho_1 c_1}{\rho_2 c_2 + \rho_1 c_1} = \frac{Z_2 - Z_1}{Z_2 + Z_1} \tag{2}$$

where R represents the ratio of reflected acoustic wave to incident acoustic wave, Z_1 is the acoustic impedance of material 1, Z_2 is the acoustic impedance of material 2, and acoustic impedance is the product of the material's wave velocity and density. For concrete materials, the acoustic impedance is 7 to 10 × 10^6kg/(m^2·s), and for air, it is 0.4 kg/(m^2·s). Therefore, it can be simply assumed that when a stress wave propagates from concrete to air, complete reflection occurs. Concrete, as a highly heterogeneous material composed of various constituents, contains voids within its structure. Consequently, when a stress wave travels through concrete, a certain degree of attenuation occurs. Additionally, due to the layer-by-layer deposition method employed in 3DPC, there are increased void ratios between layers, and a series of chemical reactions occur at the interface layer, resulting in changes in the composition. Therefore, greater attenuation of stress waves occurs between interface layers. Based on this property, we can achieve non-destructive testing of the interface bond strength of 3DPC dependent on changes in stress wave amplitude.

3.2 Experimental results

The experimental results are shown in Table 3.

Table 3: Test results

Specimen ID	Sound time (**μs**)	Average wave speed (km/s)	Amplitude (dB)	Interface bonding strength (MPa)
C-100	24.1	4.27	149.56	2.66
C-300	73.2	4.1	147.71	
3D-5	12.8	3.75	136.82	1.28
3D-6	15.0	3.8	135.45	1.48
3D-7	16.1	3.85	135.31	1.67

3D-8	20.3	3.74	134.88	1.73
3D-9	22.7	3.61	130.50	1.65
3D-10	24.4	3.89	127.79	1.53

From the experimental results, it can be observed that for 3DPC, both the propagation speed and wave amplitude are significantly lower compared to traditionally cast concrete. This can be attributed to the presence of gaps between the printed layers, which leads to a decrease in stress wave transmission speed and amplitude. As shown in Figure 2, where wave amplitude and interface strength are plotted together, it is evident that when the number of printed concrete layers increases from 5 to 8, the decrease in wave amplitude is relatively slow. However, when the number of layers increases from 8 to 10, the decrease in wave amplitude is more pronounced.

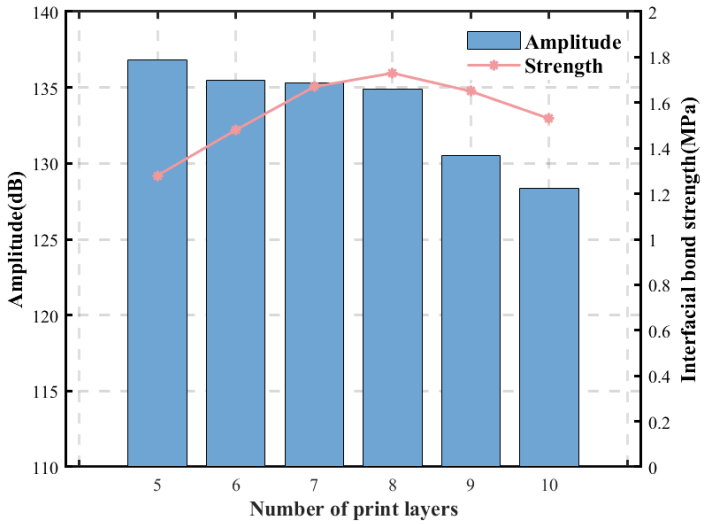

Figure 2: Number of printed layers - wave amplitude/interface bond strength

Through splitting experiments, the interface bond strength of 3DPC can be determined. When the number of printed layers increases from 5 to 8, the interface bond strength improves with the increase in layers. However, when the layers increase from 8 to 10, the bond strength decreases as the number of layers increases. This indicates that gravity affects the interface bond strength of 3DPC. Previous research has shown that slight pressure aids in the bonding between layers, while excessive pressure causes large deformations and interconnected or continuous voids at the bottom interface, significantly reducing the mechanical properties of printed concrete. Therefore, when the number of interface layers is less than 8, the bond strength increases with gravity due to insufficient bonding. However, when the number of interface layers exceeds this threshold of 8, the increased gravity leads to more defects such as voids, thereby reducing the interface bond strength.

4 MODEL AND ANALYSIS

4.1 Model description

The 3D printing process is illustrated in Figure 3. After printing one layer, the topmost concrete comes into contact with air first, leading to the earliest hydration reaction. In contrast, the concrete that has not been exposed to air hydrates more slowly. Additionally, the evaporation of moisture from the top layer reduces its water content compared to the inner concrete. The difference in reaction times results in changes in physical and chemical properties, as shown in Fig. 3(a).

Simultaneously, as subsequent layers of concrete are printed, the process of extrusion causes moisture migration due to gravity, leading to the formation of a porous structure, as shown in Fig. 3(b). At this stage, the interface layer of the 3DPC consists of the initial layer's surface concrete, the bottom concrete of the subsequent layer, and a complex porous structure. When a stress wave reaches the interface layer, the difference in acoustic impedance between the various media causes a certain degree of amplitude attenuation according to the principle of wave reflection. This results in distinctions between 3DPC and cast concrete during ultrasonic non-destructive testing. Additionally, differences in moisture content and hydration products make the bond interface the weakest part of the 3DPC.

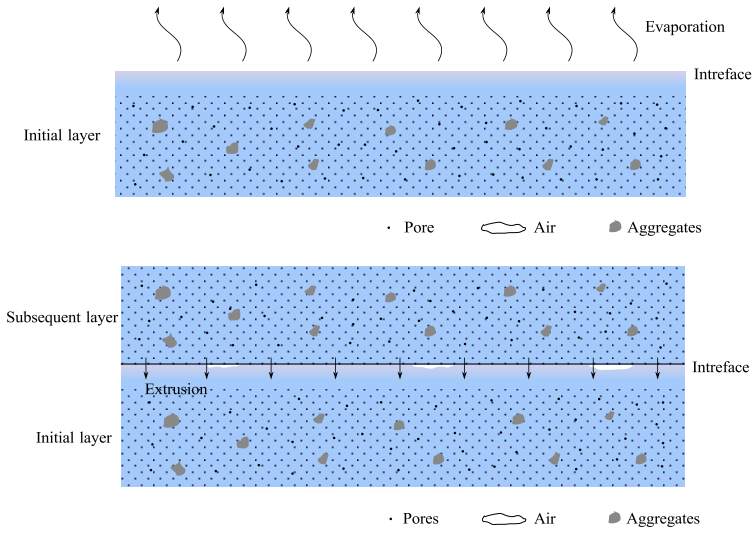

Figure 3: Formation process of the interface layer in 3D printed concrete

4.2 Amplitude loss-interface bond strength analysis

The unit of amplitude is decibels (dB), and its conversion formula can be written as:

$$A = 20\log(P_e) \tag{3}$$

where P_e represents the voltage output of the sensor.

To establish the loss equation, we introduce the concept of amplitude loss denoted by L. To correspond with the principle of wave reflection, we define the loss as:

$$P_e = \frac{P_0}{L} \tag{4}$$

where P_0 represents the voltage output of the sensor without any loss.

The attenuation of wave amplitude is divided into three parts. The first part consists of losses incurred as stress waves enter the concrete through the coupling agent and exit the concrete to the coupling agent. In a single batch of tests, the loss in this part should be constant and uniform. The second part comprises losses incurred as stress waves propagate within the concrete. This loss is proportional to the height of the concrete. The farther the stress wave travels within the concrete, the greater the loss in this part. The third part consists of amplitude losses caused by the interface layer of 3DPC. When the stress wave reaches the interface layer, reflection and transmission of the wave occur, resulting in attenuation of the first wave amplitude. Compared to the first two parts, this part also causes the largest amplitude loss. As the number of layers increases, the loss will rise exponentially. Based on this assumption, the loss caused by each interface layer L_i can be calculated, as showed in Table 4.

Table 4: Determination of amplitude loss in interface layer

Specimen ID	C-100	3D-5	3D-6	3D-7	3D-8	3D-9	3D-10
$1/L_i$	1	0.6834	0.716	0.7556	0.7826	0.7583	0.7565
Interface bond strength (MPa)	2.66	1.28	1.48	1.67	1.73	1.65	1.53

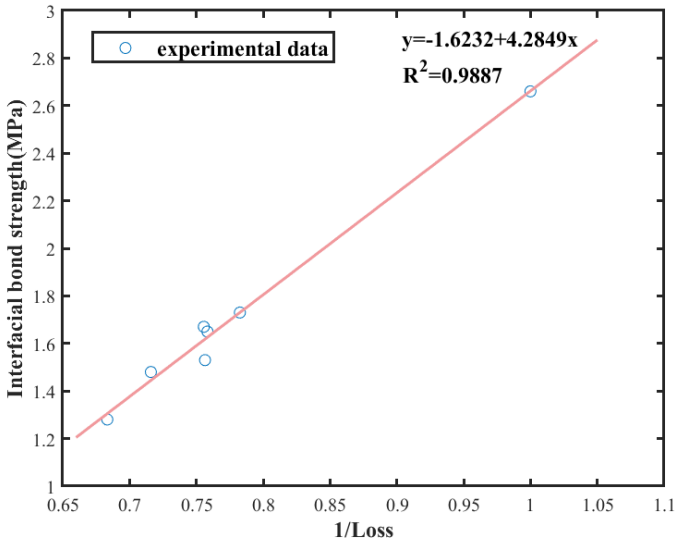

Figure 4: $1/L_i$-f_{bs} regression line

We calculated the reciprocal of the amplitude loss for each layer of the printed concrete and used it as the *X*-axis. The interface bond strength was plotted as the *Y*-axis in Figure 4. For cast concrete, the horizontal coordinate was set to 1, and the vertical coordinate was set to 2.66 MPa. It was evident that all points nearly fell on the same straight line. By fitting the data, the interface bond strength can be described as:

$$f_{bs} = -1.6232 + \frac{4.2849}{L_i} \tag{5}$$

Thus, the interface bond strength f_{bs} can be calculated based on the amplitude loss of each layer.

5 CONCLUSIONS

- The interface layers of 3DPC affect the transmission of stress waves, causing reflection and transmission of the waves, which significantly reduces the wave amplitude.
- The non-destructive testing method that relies on amplitude loss can be effectively applied to assess the interface bond strength. The lower the interface bond strength, the greater the amplitude loss, and there is a strong linear relationship between bond strength and the reciprocal of amplitude loss.
- Gravity affects the interface bond performance of printed concrete. The interface bond strength of concrete with a lower number of printed layers (5-7) and a higher number of layers (9-10) is lower compared to that with 8 layers.

REFERENCES

[1] Liu S, He Z and Hu L. Interface adhesion of fresh-on-fresh cast ultra-high performance concrete–normal concrete: Effect and mechanism of pour delay and ambient humidity. *Journal of Building Engineering*, (2023) **78**: 107679.

[2] Ding T, Xiao J and Mechtcherine V. Microstructure and mechanical properties of interlayer regions in extrusion-based 3DPC: A critical review. *Cement and Concrete Composites*, (2023) **141**: 105154.

[3] Panda B, Chandra Paul S and Jen Tan M. Anisotropic mechanical performance of 3D printed fiber reinforced sustainable construction material. *Materials Letters*, (2017) **209**: 146–149.

[4] Xiao J, Liu H and Ding T. Finite element analysis on the anisotropic behavior of 3DPC under compression and flexure. *Additive Manufacturing*, (2021) **39**: 101712.

[5] Liu H, Xiao J and Ding T. Flexural performance of 3D-printed composite beams with ECC and recycled fine aggregate concrete: Experimental and numerical analysis. *Engineering Structures*, (2023) **283**: 115865.

[6] Mechtcherine V, Bos F P, Perrot A, Da Silva W R L, Nerella V N, Fataei S, Wolfs R J M, Sonebi M and Roussel N. Extrusion-based additive manufacturing with cement-based materials – Production steps, processes, and their underlying physics: A review. *Cement and Concrete Research*, (2020) **132**: 106037.

[7] Reinold J, Nerella V N, Mechtcherine V and Meschke G. Extrusion process simulation and layer shape prediction during 3D-concrete-printing using the Particle Finite Element Method. *Automation in Construction*, (2022) **136**: 104173.

[8] Vantyghem G, De Corte W, Shakour E and Amir O. 3D printing of a post-tensioned concrete girder designed by topology optimization. *Automation in Construction*, (2020) **112**: 103084.

[9] Liu H, Xiao J and Ding T. Flexural performance of 3D-printed composite beams with ECC and recycled fine aggregate concrete: Experimental and numerical analysis. *Engineering Structures*, (2023) **283**: 115865.

[10] Şahin H G and Mardani A. How does rheological behaviour affect the interlayer-bonding strength of 3DPC mixtures? *Journal of Adhesion Science and Technology*, (2023): 1–25.

[11] Wang L, Yang Y, Yao L and Ma G. Interfacial bonding properties of 3D printed permanent formwork with the post-casted concrete. *Cement and Concrete Composites*, (2022) **128**: 104457.
[12] Zhang Y, Yang L, Qian R, Liu G, Zhang Y and Du H. Interlayer adhesion of 3DPC: Influence of layer stacked vertically. *Construction and Building Materials*, (2023) **399**: 132424.
[13] Tian J, Wu X, Zheng Y, Hu S, Du Y, Wang W, Sun C and Zhang L. Investigation of interface shear properties and mechanical model between ECC and concrete. *Construction and Building Materials*, (2019) **223**: 12–27.
[14] Geng Z, She W, Zuo W, Lyu K, Pan H, Zhang Y and Miao C. Layer-interface properties in 3DPC: Dual hierarchical structure and micromechanical characterization. *Cement and Concrete Research*, (2020) **138**: 106220.
[15] Shen Y, Lin L, Wei S, Yan J and Xu T. Research on the preparation and mechanical properties of solidified 3DPC materials. *Buildings*, (2022) **12**(12): 2264.
[16] Panda B and Tan M J. Experimental study on mix proportion and fresh properties of fly ash based geopolymer for 3D concrete printing. *Ceramics International*, (2018) **44**(9): 10258–10265.
[17] Panda B, Paul S C, Mohamed N A N, Tay Y W D and Tan M J. Measurement of tensile bond strength of 3D printed geopolymer mortar. *Measurement*, (2018) **113**: 108–116.
[18] Roussel N. Rheological requirements for printable concretes. *Cement and Concrete Research*, (2018) **112**: 76–85.
[19] Roussel N, Ovarlez G, Garrault S and Brumaud C. The origins of thixotropy of fresh cement pastes. *Cement and Concrete Research*, (2012) **42**(1): 148–157.
[20] Keita E, Bessaies-Bey H, Zuo W, Belin P and Roussel N. Weak bond strength between successive layers in extrusion-based additive manufacturing: measurement and physical origin. *Cement and Concrete Research*, (2019) **123**: 105787.
[21] Wolfs R J M, Bos F P and Salet T A M. Hardened properties of 3DPC: The influence of process parameters on interlayer adhesion. *Cement and Concrete Research*, (2019) **119**: 132–140.
[22] Kruger J, Zeranka S and Van Zijl G. 3D concrete printing: A lower bound analytical model for buildability performance quantification. *Automation in Construction*, (2019) **106**: 102904.